Hydrological cycle amplification imposes spatial pattern on climate change response of ocean pH and carbonate chemistry

Allison Hogikyan [1,2] and Laure Resplandy [3,4]

[1]Atmospheric and Oceanic Sciences Program, Princeton University, Sayre Hall, 300 Forrestal Rd, Princeton, NJ 08540, USA
[2]Department of the Geophysical Sciences, University of Chicago
[3]Geosciences Department, Princeton University, Guyot Hall, Guyot Ln., Princeton, NJ 08544, USA
[4]High Meadows Environmental Institute, Princeton University

Correspondence: Allison Hogikyan (hogikyan@uchicago.edu)

Abstract. Ocean CO_2 uptake and acidification in response to human activities are driven primarily by the rise in atmospheric CO_2, but are also modulated by climate change. Existing work suggests that this 'climate effect' influences the uptake and storage of anthropogenic carbon and acidification via the global increase in ocean temperature, although some regional responses have been attributed to changes in circulation or biological activity. Here, we investigate spatial patterns in the climate

5 effect on surface-ocean acidification (and the closely related carbonate chemistry) in an Earth System Model under a rapid CO_2-increase scenario, and identify a different driving process. We show that the amplification of the hydrological cycle, a robustly simulated feature of climate change, is largely responsible for the spatial patterns in this climate effect at the sea surface. This 'hydrological effect' can be understood as a subset of the total climate effect which includes warming, hydrological cycle amplification, circulation and biological changes. We demonstrate that it acts through two primary mechanisms: (i) directly

10 diluting or concentrating dissolved ions by adding or removing freshwater and (ii) altering the sea surface temperature, which influences the solubility of dissolved inorganic carbon (DIC) and acidity of seawater. The hydrological effect opposes acidification in salinifying regions, most notably the subtropical Atlantic, and enhances acidification in freshening regions such as the western Pacific. Its single strongest effect is to dilute the negative ions that buffer the dissolution of CO_2, quantified as 'Alkalinity'. The local changes in Alkalinity, DIC, and pH linked to the pattern of hydrological cycle amplification are as

15 strong as the (largely uniform) changes due to warming, explaining the weak increase in pH and DIC seen in the climate effect in the subtropical Atlantic Ocean.

1 Introduction

The increasing atmospheric concentration of carbon dioxide (CO_2) causes a flux of CO_2 into the ocean, typically termed the 'CO$_2$-concentration feedback' (e.g. Williams et al., 2019) (here, we will use the term 'CO$_2$ effect'). This oceanic CO_2 uptake

20 increases the total carbon content of the ocean (total dissolved inorganic carbon; DIC), decreases the availability of buffering ions (Alkalinity or Alk), and consequently leads to ocean acidification (decrease in pH: $-\log_{10}[H^+]$). This study links the enhancement of the hydrological cycle with warming to regional changes in DIC, Alkalinity, and acidification, thus linking a robust physical response of the climate system to a biological impact of climate change. Ocean acidification reduces the stabil-

ity of solid calcium carbonate, weakening the protective shells of marine organisms, with negative impacts already visible, for example on tropical coral reefs (e.g., Caldeira and Wickett, 2003; Gattuso et al., 2014). Together with other stressors, including warming and ocean de-oxygenation, acidification increases the vulnerability of certain marine organisms. For example, combined acidification and low oxygen levels narrow the range of temperatures at which organisms can function, and warming tends to increase baseline metabolic rates, further narrowing this thermal window (e.g., Pörtner, 2012; Doney et al., 2020; Kroeker et al., 2013).

Chemical changes in DIC, Alkalinity and pH are also modulated by climate change, via warming, circulation, freshwater flux, and biological changes. These effects can be isolated from the direct CO_2 effect as a separate 'carbon-climate feedback' (here we will use the term 'climate effect', including all changes other than the atmospheric CO_2 increase, i.e. temperature, circulation, freshwater flux, and biological). This 'climate effect' has been shown to decrease global CO_2 uptake and storage by approximately 10% in projections of high carbon emissions scenarios (Arora et al., 2013; Friedlingstein and Prentice, 2010; Williams et al., 2019; McNeil and Matear, 2007; Schwinger et al., 2014). The best understood facet of the climate effect on seawater chemistry is warming, which drives a decrease in anthropogenic carbon uptake due to weakened solubility and ventilation (Katavouta and Williams, 2021). However, Katavouta and Williams (2021) also note that some regional patterns cannot be accounted for by these two processes, and indeed other studies have suggested that more complex shifts in circulation patterns and changes in biological activity contribute to regional climate effects on carbon storage in the interior (e.g. Lovenduski et al., 2008; Siedlecki et al., 2021; Pilcher et al., 2019). Although these studies demonstrate that regional variations in the climate effect are not exclusively related to warming, they are focused on anthropogenic carbon uptake and do not address the net effect of DIC and Alkalinity changes on regional ocean acidification. McNeil and Matear (2007) describe the climate effect on ocean acidification and point out that warming has a direct effect to decrease pH and an indirect effect to decrease the solubility of CO_2, which limits acidification. They find that the net of these direct and indirect effects is small on global average, but did not address the larger regional responses, which are critical for anticipating ecosystem impacts. Here, we find that the amplification of the hydrological cycle with warming, a robust response of climate models to global warming which has recently been linked to patterns of ocean oxygen loss with climate change (Hogikyan et al., 2024), is in fact responsible for the bulk of the spatial pattern in surface ocean DIC and Alkalinity and consequently acidification attributed to the climate effect.

The 'hydrological cycle amplification' reinforces sea surface salinity (SSS) patterns, leading to a 'salty-get-saltier, fresh-get-fresher' rule of thumb for changes in SSS, especially at low and mid-latitudes where the hydrological cycle is strongest (Durack and Wijffels, 2010). Specifically, hydrological cycle amplification refers to enhanced spatial patterns of net air-sea freshwater fluxes (precipitation-evaporation) which are largely responsible for the mean SSS patterns (Held and Soden, 2006; Manabe and Wetherald, 1975). Hydrological cycle amplification can induce regional patterns in surface seawater carbonate chemistry in two ways. First, freshwater fluxes can directly change the concentration of dissolved species, potentially increasing the concentrations of DIC and Alkalinity in 'salty-get-saltier' regions and decreasing their concentrations in 'fresh-get-fresher' regions. pH increases with DIC and decreases with Alkalinity, so that freshwater fluxes drive a small net change in pH. Second, these changes in salinity modify the ocean circulation and lead to a net increase in ocean heat uptake globally, which weakens

surface warming (as shown by Liu et al., 2021; Williams et al., 2007). This heat uptake is due to enhanced subduction in regions of sea surface strong salinity increase, primarily the North Atlantic. This relative cooling could drive an increase in DIC and pH, weakening the influence of warming in the total climate effect.

We estimate the regional DIC, Alkalinity, and pH changes due to (a) the total climate effect and (b) the subset of the climate effect due only to hydrological cycle amplification- the 'hydrological effect'- using a high-CO_2-increase scenario in a global Earth System Model (NOAA-GFDL's ESM2M; Dunne et al. (2013)). The experiments follow those used to isolate the hydrological effect on ocean oxygen loss in Hogikyan et al. (2024). We focus on the sea surface, where the response to hydrological cycle amplification is largest, and separate the surface into a 'fresh-get-fresher' and a 'salty-get-saltier' regime; the changes in these two regimes largely cancel in the global average but could modify local carbonate chemistry and its biological impacts. Then, we further attribute the climate effect and hydrological effect DIC, Alkalinity, and pH changes to two primary mechanisms: (a) freshwater (dilution and concentration of DIC and Alkalinity), and (b) thermal (temperature-driven) effects. We find that hydrological cycle amplification can account for much of the regional pattern in the total climate effect, since it is the sole driver of long-term trends in freshwater fluxes, while temperature changes are more spatially uniform. We show that these freshwater fluxes change the concentration of Alkalinity slightly more than that of DIC due to the mean chemistry of the ocean, with the consequence that DIC, and pH tend to increase along with Alkalinity in 'salty-get-saltier' regions and decrease in 'fresh-get-fresher' regions.

2 Methods

2.1 Earth System Model and experiments to isolate hydrological and climate effects

We use the Geophysical Fluid Dynamics Laboratory Earth System Model 2M (ESM2M), which is fully described in Dunne et al. (2012, 2013). The version of ESM2M used here (public release 5.0.2) uses the atmosphere model AM2 with a horizontal resolution of approximately 50 km, and ocean model MOM5 with a horizontal resolution of approximately 100km, as well as the land model LM3.0 and ocean biogeochemical model TOPAZ2. In order to isolate the signature of increasing atmospheric CO_2 and the associated amplification of the hydrological cycle, we force the model with a strong atmospheric CO_2 increase of 1% per year, beginning from the pre-industrial concentration of 286 ppm, until the CO_2 level doubles after 70 years. During years 71-100 the CO_2 level is held fixed at double the pre-industrial concentration (562 ppm), so that the entire experiment is 100 years long. We compare three different experiments with this 1%-to-doubling CO_2 forcing. This is identical to the experimental setup used in Hogikyan et al. (2024), and further details can be found therein. The spatial patterns of salinity changes agree with long-term trends in observations and other climate models.

In the first experiment, the model freely responds to the prescribed atmospheric CO_2 ('Standard'), and the strength of the hydrological cycle intensifies with warming, amplifying patterns of freshwater fluxes and SSS. In the second experiment, SSS is nudged towards its pre-industrial monthly climatology with a restoring flux of freshwater ('Fix-SSS') as CO_2 increases along the same 1%-to-doubling trajectory. There is no restoring under seasonal sea ice. The freshwater restoring flux dilutes (or concentrates) all chemical species, although SSS is used to determine its strength. The difference between the Standard and
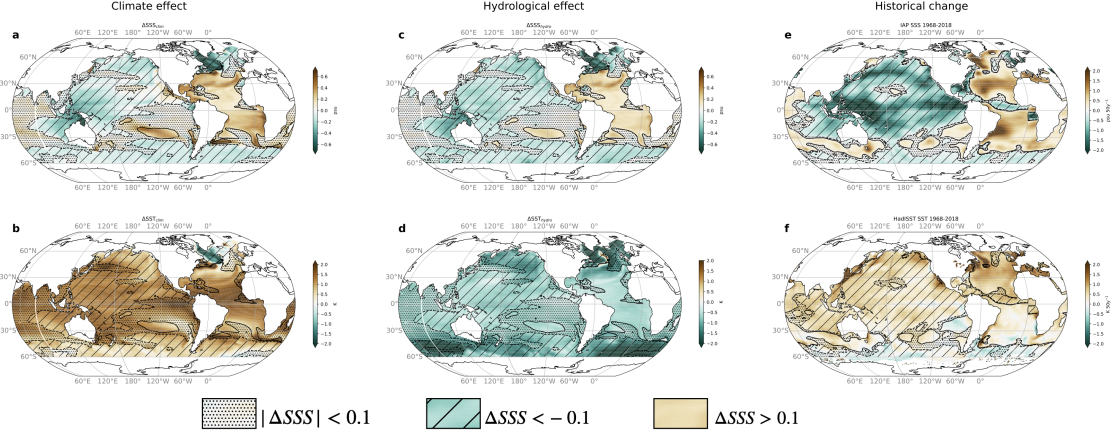
Figure 1. Sea surface salinity (SSS) and temperature (SST) changes associated with climate and hydrological effects. (a, b) SSS and SST change with climate effect (Standard minus Fix-Clim experiments) which includes hydrological effect and other changes, notably global warming; (c, d) SSS and SST change with hydrological effect (Standard minus Fix-SSS experiments) which weakens surface warming and reinforces SSS patterns. Also shown for comparison is the recent historical linear trend pattern in (e) SSS and (f) SST, as quantified by the IAP reanalysis (Cheng et al., 2017) and the HadISST analysis product (Rayner et al., 2003). Stippling indicates regions where ΔSSS_{hydro} is small ($|\Delta SSS_{hydro}| < 0.1$ psu); these regions are excluded from our analysis. Hatching indicates the fresh-get-fresher regime where $\Delta SSS_{hydro} < -0.1$ psu. A lack of hatching indicates the salty-get-saltier regime where $\Delta SSS_{hydro} > +0.1$ psu. See Table 1 for description of experiments.

Fix-SSS experiments provides an estimate of the impact of the hydrological cycle amplification on the ocean (including the direct freshwater flux and ocean circulation adjustment), and for a given variable X we define the change due to hydrological cycle amplification, the 'hydrological effect', in terms of the difference between these two simulations:

$$\Delta X_{hydro} = X_{Standard} - X_{Fix-SSS}$$

To contextualize the hydrological effect as a part of the total carbon-climate feedback, or 'climate effect', we also run a 'Fixed-Climate' experiment in which the same 1% to doubling atmospheric CO_2 increase interacts with ocean biogeochemistry but not with radiation so that there is no global warming (no change in climate). In this experiment, the ocean experiences carbon uptake due to atmospheric CO_2 increase, but no warming or hydrological cycle amplification. The climate effect can therefore be defined by

$$\Delta X_{clim} = X_{Standard} - X_{Fix-Clim}$$

(as in e.g. Williams et al., 2007, 2019; Katavouta and Williams, 2021). In this framework, we define $X_{Standard}$, $X_{Fix-Clim}$ and $X_{Fix-SSS}$ using the average over the last 30 years of each simulation (years 71-100) when atmospheric CO_2 is held steady at double the pre-industrial concentration and the system is beginning to equilibrate at this higher CO_2 level, to decrease the influence of internal variability or rapid adjustments to forcing. Results are presented for the Atlantic, Indian, and Pacific Oceans, with a focus on the low- and mid-latitudes where the hydrological cycle is most active, i.e. where the amplification

90

of evaporation/precipitation patterns is strongest. We ignore high latitudes where the surface freshwater balance is instead dominated by ice-ocean interactions (north of 55°S and with a mask applied where seasonal sea ice is found in the pre-industrial control run; see mask in Figure 1).

95   ΔX_{clim} includes a contribution from ΔX_{hydro} as well as from other changes. For instance, the climate effect includes a significant surface warming, so that ΔSST_{clim} is positive (i.e., $SST_{Standard}$ exceeds $SST_{Fix-Clim}$ at the end of the simulation,Figure 1c). However, the hydrological cycle amplification moderates surface warming by enhancing ocean heat uptake (Williams et al., 2007; Liu et al., 2021), so that ΔSST_{hydro} is negative (i.e., $SST_{Standard}$ is less than $SST_{Fix-SSS}$ at the end of the simulation, Figure 1d).

100   All model experiments, and the abbreviations we use to reference them, are summarized in Table 1.

2.2   Freshwater and thermal contributions to DIC and Alkalinity changes

We quantify the influence of freshwater fluxes (dilution/concentration of DIC and Alkalinity) and temperature changes on DIC and Alkalinity in both the hydrological effect (the amplification of the hydrological cycle, represented by the Standard - Fix-SSS experiments) and the climate effect (the total effect of climate change including warming, hydrological cycle amplification,

105   etc., represented by the Standard - Fix-Clim experiments).

DIC is affected by both freshwater fluxes and temperature changes, so that we can decompose ΔDIC_{hydro} as follows:

$$\Delta DIC_{hydro} = \Delta DIC_{FW,hydro} + \Delta DIC_{thermal,hydro} + R_{DIC,hydro}$$

where $\Delta DIC_{FW,hydro}$ and $\Delta DIC_{thermal,hydro}$ correspond to contributions from dilution or concentration by freshwater fluxes (FW) and changes due to a temperature change (thermal). The residual R includes all other processes that affect DIC and Alkalinity (e.g., air-sea fluxes of CO_2, calcium carbonate precipitation/dissolution, production and remineralization of organic matter, and salinity) as well as co-variations between the thermal and freshwater effects and errors in our method of

110   estimating these effects (which are elaborated on below).

In contrast, Alkalinity does not vary with temperature. Its hydrological effect can be approximated as:

$$\Delta Alk_{hydro} = \Delta Alk_{FW,hydro} + R_{Alk,hydro}$$

We can attribute the total climate effect in DIC and Alkalinity to freshwater and thermal effects, following the same framework:

$$\Delta DIC_{clim} = \Delta DIC_{FW,clim} + \Delta DIC_{thermal,clim} + R_{DIC,clim}$$

$$\Delta Alk_{clim} = \Delta Alk_{FW,clim} + R_{Alk,clim}$$

The various residuals R are quantified in Figures A1 and A2. We are largely successful in reconstructing the hydrological effect, and R is generally small relative to ΔDIC_{hydro} and ΔAlk_{hydro} (error <5 μmol/kg at a point relative to broad regional changes of 15-40 μmol/kg; Figures 2, A1. Note AX indicates Appendix Figure X). The error is somewhat more significant in reconstructing the climate effect (ΔDIC_{clim} and ΔAlk_{clim}, Figure A2), especially for DIC (error <8 μmol/kg). This is most

115 likely due to the fact that the climate effect leads to anomalous air-sea CO_2 fluxes (primarily due to warming, but possibly also influenced by circulation changes) which change DIC and can indirectly lead to changes in Alkalinity.

We quantify the effect of freshwater fluxes on Alkalinity and DIC ($\Delta Alk_{FW,hydro}$, $\Delta DIC_{FW,hydro}$) with a simple conservation argument which neglects the effects of mixing and advection, a fair approximation within the mixed layer. In this case, DIC, Alkalinity, and salt are diluted/concentrated by air-sea freshwater fluxes by the same fraction $f_{FW,hydro} = \Delta S_{hydro}/S_{Fix-SSS}$

120 referenced to salinity (S). For example, if a freshwater flux into the surface in the Standard warming experiment diluted SSS by $f_{FW,hydro} = 5\%$ compared to the Fix-SSS experiment (i.e., $SSS_{Standard} = 0.95\ SSS_{Fix-SSS}$), then surface DIC and Alkalinity would also be diluted by $f_{FW,hydro} = 5\%$ from the reference Fix-SSS concentrations ($DIC_{Standard} = 0.95\ DIC_{Fix-SSS}$; $Alk_{Standard} = 0.95\ Alk_{Fix-SSS}$). We can therefore approximate $\Delta DIC_{FW,hydro}$ and $\Delta Alk_{FW,hydro}$ as:

$$\begin{aligned}
\Delta Alk_{FW,hydro} &= f_{FW,hydro}\ Alk_{Fix-SSS}, \\
\Delta DIC_{FW,hydro} &= f_{FW,hydro}\ DIC_{Fix-SSS}
\end{aligned} \tag{1}$$

125 The effects of mixing and transport on salinity are included in f_{FW}, because it is derived from changes in salinity. However, since mixing and transport act on different spatial gradients for each variable, f_{FW} cannot be expected to be the same for salinity, DIC, Alk, etc., except in the mixed layer where gradients are relatively weak for all constituents. As a consequence, we restrict our analysis to the mixed layer, where this error is very small relative to the changes driven by temperature and freshwater effects (as demonstrated in Figures 3 and A1, A2).

We estimate DIC changes due to thermal changes following Sarmiento (2006), using a constant thermal sensitivity $\frac{\partial DIC}{\partial T}$ of $-7\ \frac{\mu mol/kg}{K}$:

$$\Delta DIC_{thermal,hydro} = \frac{\partial DIC}{\partial T}\Delta T_{hydro} = -7\Delta T_{hydro}$$

130 This approximation introduces some error since $\frac{\partial DIC}{\partial T}$ is not constant, but we find that our results do not change if we allow the sensitivity to vary at each model grid point and month. Our conclusions are not sensitive to the choice of constant within a range of $7\pm2\ \frac{\mu mol/kg}{K}$.

The decomposition of DIC and Alk changes laid out above is also summarized in Table 2.

2.3 Attribution of surface pH changes to hydrological and climate effects

135 Equilibrium pH can be understood as a nonlinear function of DIC, Alkalinity, temperature (T), and salinity (S), so that a difference in pH between two model experiments or ocean chemical states can be interpreted in terms of the corresponding changes in DIC, Alkalinity, temperature, and salinity between these two states (as in e.g. García-Ibáñez et al., 2016). An increase in DIC due to CO_2 dissolution produces H^+ ions and decreases pH, whereas an increase in Alkalinity represents a greater seawater buffering capacity and yields a higher pH. Temperature has a direct negative relationship with pH (warming ionizes water, thus

140 decreasing pH), and an indirect positive relationship with pH (the solubility of DIC decreases with temperature and leads to an increase in pH). Salinity has a small effect on pH and will not be discussed in this study.

We define the 'hydrological effect' and 'climate effect' on pH as:

$$\Delta pH_{hydro} = pH(DIC_{Std}, Alk_{Std}, T_{Std}, S_{Std}) - pH(DIC_{Fix-SSS}, Alk_{Fix-SSS}, T_{Fix-SSS}, S_{Fix-SSS}) \tag{2}$$

$$\Delta pH_{Clim} = pH(DIC_{Std}, Alk_{Std}, T_{Std}, S_{Std}) - pH(DIC_{Fix-Clim}, Alk_{Fix-Clim}, T_{Fix-Clim}, S_{Fix-Clim}) \tag{3}$$

where the 'Standard' as well as 'Fix-SSS', 'Fix-Clim' pH are all estimated using the marine carbonate chemistry solver PyCO2SYS (Humphreys et al., 2022) to remove any biases between CO2SYS and the earth system model. pH is a highly non-linear function of other state variables, and is solved for iteratively. We therefore make use of this established solver rather than making our own estimate, as we do for DIC and Alk. These ΔpH_{Clim} and ΔpH_{Hydro} estimates from CO2SYS are not identical to $pH_{Std} - pH_{Fix-Clim}$ and $pH_{Std} - pH_{Fix-Hydro}$ from the model experiments because CO2SYS assumes chemical equilibrium. (As a point of interest, ESM2M is constrained by the conservation of heat and mass in the coupled model but a given location is not necessarily in chemical equilibrium). We use this method because it allows us to break down ΔpH_{hydro} and ΔpH_{Clim} into freshwater (chemical dilution) and thermal (temperature-driven) components (as well as a residual due to errors in method and other drivers). The changes in pH are attributed to freshwater and thermal effects, similarly to DIC and Alkalinity:

$$\Delta pH_{hydro} = \Delta pH_{FW,hydro} + \Delta pH_{thermal,hydro} + R$$

Freshwater fluxes affect pH primarily through their effect on DIC and Alkalinity; we use the DIC and Alkalinity changes due to freshwater fluxes (as estimated in section 2.2) to evaluate the freshwater flux effect on pH ΔpH_{FW}. The principle here is to take our estimates of the change in DIC and Alkalinity due to freshwater fluxes and see what pH change is predicted to result (isolating the freshwater effect and ignoring other changes, e.g. temperature). More specifically, $\Delta pH_{FW,hydro}$ is defined as the difference between the theoretical pH with diluted/concentrated DIC and Alk (in bold) and and the reference $pH_{Fix-SSS}$ which excludes the influence of hydrological cycle amplification:

$$\Delta pH_{FW,hydro} = pH((\mathbf{f_{FW,hydro} + 1})\mathbf{DIC_{Fix-SSS}}, (\mathbf{f_{FW,hydro} + 1})\mathbf{Alk_{Fix-SSS}},$$
$$SST_{Fix-SSS}, SSS_{Fix-SSS}) - pH_{Fix-SSS}$$

We next want to ask what pH change should result from the temperature changes. However, we know that thermal changes in DIC (which we estimate above) co-occur with actual temperature changes which also have a direct influence on pH. We define the thermally driven change in pH ($\Delta pH_{thermal}$) to include these direct and indirect thermal effects (SST and DIC changes, respectively, emphasized in bold):

$$\Delta pH_{thermal,hydro} = pH(\mathbf{DIC_{Fix-SSS} + \Delta DIC_{thermal,hydro}}, Alk_{Fix-SSS},$$
$$\mathbf{SST_{Standard}}, SSS_{Fix-SSS}) - pH_{Fix-SSS}$$

The decomposition of pH changes laid out above is also summarized in Table 3.

Table 1. Simulation definitions

Standard	CO_2 increases at 1% per year from 286 to 572 ppm (requires 70 years) then is held at 572 ppm for another 30 years, for 100 total simulation years
Fix-SSS	CO_2 trajectory is as in the Standard experiment, and SSS is restored to pre-industrial concentrations
Fix-Clim	Model is heated following the CO_2 trajectory of the Standard experiment, but additional CO_2 does not interact with model chemistry (e.g. there is no ocean carbon uptake)

Table 2. ΔDIC, ΔAlk component definitions. X stands for DIC and Alk.

ΔX_{Hydro}	Change in X due to hydrological cycle amplification (averaged over simulation years 71-100)	$\Delta X_{Hydro} = X_{Standard} - X_{Fix-SSS}$ $\Delta X_{Hydro} = \Delta X_{FW,hydro} + \Delta X_{therm,hydro} + \text{residual}_{hydro}$
ΔX_{Clim}	Change in X due to climate effect (averaged over simulation years 71-100)	$\Delta X_{Clim} = X_{Standard} - X_{Fix-Clim}$ $\Delta X_{Clim} = \Delta X_{FW,clim} + \Delta X_{therm,clim} + \text{residual}_{clim}$
$\Delta X_{FW,Hydro}$	Change in X due to dilution/concentration from hydrological effect	$\Delta X_{FW} = f_{FW} \cdot X_{Fix-SSS}$ where $f_{FW} = \frac{SSS_{Standard} - SSS_{Fix-SSS}}{SSS_{Fix-SSS}}$
$\Delta X_{FW,Clim}$	Change in X due to dilution/concentration from climate effect	$\Delta X_{FW} = f_{FW} \cdot X_{Fix-Clim}$ where $f_{FW} = \frac{SSS_{Standard} - SSS_{Fix-Clim}}{SSS_{Fix-Clim}}$
$\Delta DIC_{thermal,Hydro}$	Change due to temperature change from hydrological effect, undefined for Alk	$-7\frac{\mu mol/kg}{K} \cdot (SST_{Standard} - SST_{Fix-SSS})$
$\Delta DIC_{thermal,Clim}$	Change due to temperature change from climate effect, undefined for Alk	$-7\frac{\mu mol/kg}{K} \cdot (SST_{Standard} - SST_{Fix-Clim})$

3   Results

3.1   Climate-driven DIC and Alkalinity changes explained by hydrological effect

The climate model used here, ESM2M, responds to a CO_2 increase with a surface warming and enhancement of mean salinity patterns. This results in a salinity increase in salty subtropical regions (enhanced in the Atlantic, relative to the Pacific), and a decrease in fresh regions, most notably high latitudes and the western tropical Pacific Ocean (Figure 1a, b). These changes represent the 'climate effect' in SST and SSS, and are consistent with many prior studies (most notably Manabe and Wetherald, 1975; Held and Soden, 2006). Similar changes in both SST and SSS are seen in historical trends (Figure 1e, f; see Durack and Wijffels (2010)). While this 'climate effect' has been studied, and hydrological cycle amplification is known to be a robust feature, the effect of hydrological cycle amplification ('hydrological effect') has only been isolated more recently in Williams

Table 3. ΔpH component definitions.

ΔpH_{Hydro}	Change in pH due to hydrological cycle amplification using CO2SYS	CO2SYS-based pH from Standard variables minus CO2SYS-based pH from Fix-SSS variables. $\Delta\text{pH}_{Hydro} = \Delta\text{pH}_{FW,Hydro} + \Delta\text{pH}_{therm,Hydro} + \text{residual}_{Hydro}$
ΔpH_{Clim}	Change in pH due to climate effect using CO2SYS	CO2SYS-based pH from Standard variables minus CO2SYS-based pH from Fix-Clim variables. $\Delta\text{pH}_{Clim} = \Delta\text{pH}_{FW,Clim} + \Delta\text{pH}_{therm,Clim} + \text{residual}_{Clim}$
$\Delta\text{pH}_{FW,Hydro}$	Change in pH due to dilution/-concentration from hydrological effect using CO2SYS	CO2SYS-based pH from Fix-SSS variables + $\Delta X_{FW,Hydro}$ ($\text{DIC}_{Fix-SSS} + \Delta\text{DIC}_{FW,Hydro}$, $\text{Alk}_{Fix-SSS} + \Delta\text{Alk}_{FW,Hydro}$, $\text{SST}_{Fix-SSS}$, $\text{SSS}_{Fix-SSS}$) minus CO2SYS-based $\text{pH}_{Fix-SSS}$
$\Delta\text{pH}_{FW,Clim}$	Change in pH due to dilution/-concentration from climate effect using CO2SYS	CO2SYS-based pH from Fix-Clim + $\Delta X_{FW,Clim}$ ($\text{DIC}_{Fix-Clim} + \Delta\text{DIC}_{FW,Clim}$, $\text{Alk}_{Fix-Clim} + \Delta\text{Alk}_{FW,Clim}$, $\text{SST}_{Fix-Clim}$, $\text{SSS}_{Fix-Clim}$) minus CO2SYS-based $\text{pH}_{Fix-Clim}$
$\Delta\text{pH}_{thermal,Hydro}$	Change in pH due to temperature change from hydrological effect using CO2SYS	CO2SYS-based pH from Fix-SSS variables + $\Delta\text{DIC}_{thermal,Hydro}$ ($\text{DIC}_{Fix-SSS} + \Delta\text{DIC}_{thermal,Hydro}$, $\text{Alk}_{Fix-SSS}$, $\text{SST}_{Standard}$, $\text{SSS}_{Fix-SSS}$) minus CO2SYS-based $\text{pH}_{Fix-SSS}$
$\Delta\text{pH}_{thermal,Clim}$	Change in pH due to temperature change from climate effect using CO2SYS	CO2SYS-based pH from Fix-Clim variables + $\Delta\text{DIC}_{thermal,Clim}$ ($\text{DIC}_{Fix-Clim} + \Delta\text{DIC}_{thermal,Clim}$, $\text{Alk}_{Fix-Clim}$, $\text{SST}_{Standard}$, $\text{SSS}_{Fix-Clim}$) minus CO2SYS-based $\text{pH}_{Fix-Clim}$

et al. (2007); Liu et al. (2021); Hogikyan et al. (2024). As has been shown in these prior studies, the hydrological effect accounts
170 almost exactly for the SSS changes in the climate effect. It also leads to a surface cooling (due to enhanced global ocean heat
uptake) (Figure 1c, d). Please see Table 1 and the Methods section for an overview of the experiments we use to isolate the
climate effect and hydrological effect.

We next assess the climate and hydrological effects on surface carbonate chemistry. For simplicity and clarity, we average
over 'saltier' and 'fresher' ocean surface areas: specifically, where salinification is in excess of 0.1 psu (the (sub)tropical
175 Atlantic and southeast Pacific Oceans) and where freshening is stronger than -0.1 psu (the high-latitude Atlantic and remainder
of the Indo-Pacific Oceans, Figures 2, 1). Although the DIC change has a similar spatial pattern as Alkalinity, dictated by
the sign of freshwater fluxes, we will show that its magnitude is modulated by a thermal component (warming in the climate
effect and cooling in the hydrological effect). Where SSS increases, DIC is less sensitive than Alk to the climate effect (
$\Delta\text{DIC}_{clim} = +2\ \mu\text{mol/kg}$ and $\Delta\text{Alk}_{clim} = +16\ \mu\text{mol/kg}$; see Table 2 for definitions), but they have the same sensitivity to the
180 hydrological effect ($\Delta\text{DIC}_{hydro} = +16\ \text{umol/kg}$ and $\Delta\text{Alk}_{hydro} = +14\ \text{umol/kg}$). Where SSS decreases, the two have a similar
response to the climate effect ($\Delta\text{DIC}_{clim} = -13\ \text{umol/kg}$ while $\Delta\text{Alk}_{clim} = -10\ \text{umol/kg}$, black empty bars in Figure 2), but
DIC is less sensitive than Alk to the hydrological effect ($\Delta\text{DIC}_{hydro} = -5\ \text{umol/kg}$ and $\Delta\text{Alk}_{hydro} = -12\ \text{umol/kg}$, grey bars
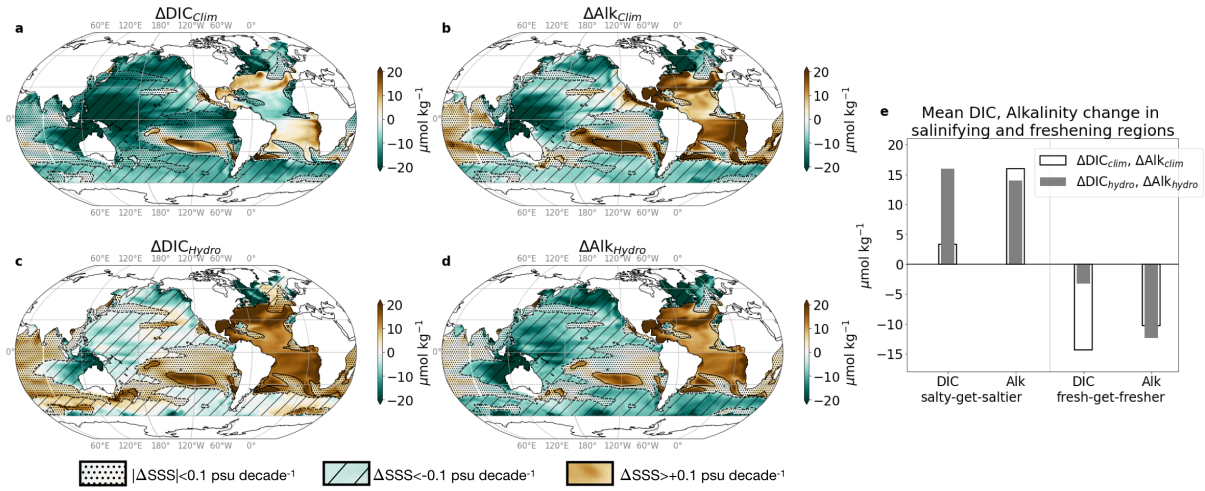
Figure 2. DIC and Alkalinity response to climate and hydrological effects. Change in surface (a) DIC and (b) Alkalinity due to the climate effect (Standard minus Fix-Clim experiments); change in surface (c) DIC and (d) Alkalinity due to the hydrological effect (Standard minus Fix-SSS experiments). (e) Mean change in DIC (black) and Alkalinity (grey) in salinifying ($\Delta SSS_{hydro} > 0.1$ psu) and freshening ($\Delta SSS_{hydro} < $ -0.1 psu) regions shown in Figure 1. For a-d, stippled areas experience nearly zero change in salinity ($|\Delta SSS_{hydro}| < 0.1$ psu) and are ignored in our analysis, while fresh-get-fresher regions are hatched ($\Delta SSS_{hydro} < $ -0.1 psu), and salty-get-saltier regions have no hatching ($\Delta SSS_{hydro} > $ +0.1 psu). See Table 2 for definitions.

in Figures 2e and 3). We can understand what controls these changes in DIC and Alkalinity by attributing them to freshwater (dilution/concentration), thermal, and residual (e.g. approximations in f_{FW}, as well as biological and circulation) effects using simple sensitivity estimates described in the Methods section.

The effect of freshwater fluxes is very similar in both the hydrological effect and the climate effect, consistent with the understanding that hydrological cycle amplification accounts for the bulk of salinity changes in the total climate effect (Durack et al., 2012) (Figure 1a, c; i.e. $f_{FW,hydro} \approx f_{FW,clim}$). However, the higher mean concentration of Alkalinity makes Alkalinity more sensitive to freshwater addition and removal than DIC (in both the total climate effect and hydrological effect; blue bars in Figure 3, maps in Figure A3). For example, when we evaluate ($\Delta X_{FW,hydro} = X_{Fix-SSS} \ f_{FW,hydro}$), $\Delta Alk_{FW,hydro}$ is slightly greater than $\Delta DIC_{FW,hydro}$ due to the greater reference $Alk_{Fix-SSS}$ (Figure 3 blue bars). The freshwater effect in salty-get-saltier waters increases DIC and Alkalinity by 17 and 19 umol/kg in the climate effect; the increase is slightly less in the hydrological effect, 12 and 14 umol/kg. Dilution from freshening decreases DIC and Alkalinity by -9 and -10 umol/kg in the climate effect. The freshwater effect on both DIC and Alk is slightly larger in the hydrological effect alone, -13 and -14 umol/kg. These discrepancies between the hydrological and climate effects are primarily due to the discrepancy between dilution/concentration fractions $f_{FW,hydro}$ and $f_{FW,clim}$, which arise from the difference in ocean circulation and salinity fields between the Fix-SSS and Fix-Clim experiments.

Changes in surface temperature substantially modify the DIC response to both the total climate effect and the hydrological effect since the solubility of DIC decreases with increasing temperature. Alkalinity, however, is not sensitive to temperature, and as a result its changes are well accounted for by the freshwater effect alone (yellow residual bars for Alk are much smaller than freshwater and total Alk changes; Figure 3). Surface warming in the climate effect decreases DIC concentrations everywhere (by -9 umol/kg in salinifying and -7 umol/kg in freshening regions), while surface cooling in the hydrological effect increases DIC concentrations everywhere (by +5 umol/kg in salinifying and +7 umol/kg in freshening regions; Figure 3 green bars). Overall, the SST and corresponding DIC changes are similar across salinifying and freshening regions (Figures 1c, d and A3b, e), although circulation changes lead to some spatial patterns in the temperature response. For example, the weaker $\Delta DIC_{thermal,clim}$ in freshening, relative to salinifying, regions (-6 vs. -8 umol/kg; Figure 3) is a consequence of the SST decrease (and positive $\Delta DIC_{thermal,clim}$) in the Labrador Sea associated with a weakening of the overturning circulation, a common transient response of climate models to global warming and North Atlantic freshening (Figure 1) (Menary and Wood, 2018; Manabe and Stouffer, 1995). Similarly, the greater $\Delta DIC_{thermal,hydro}$ in freshening regions (+7 vs. +5 umol/kg; Figure 3) is a consequence of slightly stronger cooling at high latitudes where deep isopycnal mixing enhances the surface temperature response, while the cooling in the salty (sub)tropics is weaker. Despite these small differences, the $\Delta DIC_{thermal,hydro}$ and $\Delta DIC_{thermal,clim}$ are uniform in sign and quite similar in magnitude in both regimes, leading to a contrast between the net climate and hydrological effects where $\Delta DIC_{clim} < \Delta Alk_{clim}$, while $\Delta DIC_{hydro} > \Delta Alk_{hydro}$ (black empty and filled bars in Figure 3). In summary, the sign and spatial pattern of DIC and Alkalinity changes in both the climate effect and hydrological effect are determined by freshwater fluxes associated with hydrological cycle amplification, and the magnitude of DIC changes is further modulated by changes in SST.

This simple decomposition into freshwater and thermal effects leaves some of the simulated changes in DIC and Alkalinity unexplained (with the residual error represented by the yellow bars in Figure 3). Major processes that are not included in these freshwater and thermal effects include air-sea CO_2 fluxes and other adjustments of the carbonate system, spatial shifts in the atmospheric and oceanic circulations, and biological activity. Errors in our method are also included in the residual. Despite these omissions, the decomposition skillfully reconstructs the hydrological effect in both DIC and Alkalinity ($R_{hydro} <2$ umol/kg for both; see also Figure A4), while residuals for the climate effect are slightly larger ($R_{clim} \approx$ 4-5 umol/kg for Alk and DIC; see also Figure A4). Biases in Alkalinity reconstruction are <10% of the total hydrological effect, suggesting that this simple estimate of dilution is a fairly effective estimate of the influence of hydrological cycle amplification on Alkalinity. The residuals in DIC are broadly consistent with the influence of air-sea CO_2 fluxes. For instance, the decomposition of the hydrological effect for DIC is biased slightly high in salty-get-saltier regions, consistent with unaccounted-for CO_2 outgassing (a secondary effect of the DIC increase and thus pCO_2 increase), and the inverse is true in fresh-get-fresher regions (Figure A5). Similarly, the negative bias (missing carbon) in the climate effect reconstruction in salinifying regions is consistent with anomalous CO_2 uptake linked to the decrease in DIC (Figure A5). We were not able to develop a simple attribution of surface DIC changes to air-sea fluxes (as we can with freshwater fluxes and temperature changes) because the DIC change due to a given surface flux is sensitive to multiple factors, including the effects of mixing and advection, as well as the temperature, surface wind speed, and sea state.
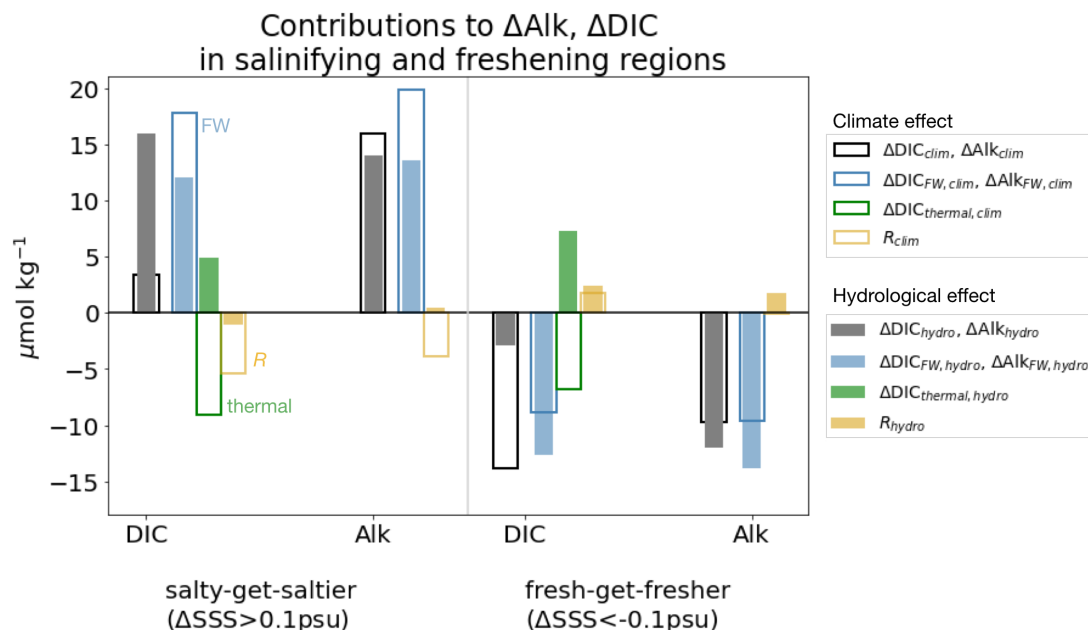
Figure 3. Thermal and freshwater components of DIC and Alkalinity changes in 'fresh-get-fresher' and 'salty-get-saltier' regions.
Change in surface DIC and Alkalinity concentrations in response to the the climate effect (empty bars) and the hydrological effect (filled bars) in salinifying and freshening regions (as in Figures 4c and 2e). Black and grey bars represent total Δ_{clim} and Δ_{hydro}, and are identical to those in Figure 2e. Blue bars represent change in DIC or Alkalinity due to freshwater fluxes. Green bars represent change in DIC due to SST change. See Table 2 for definition of components.

3.2 Acidification weakened in 'salty-get-saltier' regions and exacerbated in 'fresh-get-fresher' regions

The climate effect tends to decrease surface pH, thereby re-inforcing the acidification associated with the rise in atmospheric

235   CO_2 ($\Delta pH_{clim} <0$; Figure 4a; see Methods and Table 3 for definition of all ΔpH terms). We find, however, that on average, the climate effect enhances acidification more in 'fresh-get-fresher' regions than in 'salty-get-saltier' regions (-0.005 vs. -0.001; black empty bars in Figure 4c). The hydrological effect (dilution/concentration of DIC/Alk, direct and indirect effect of SST decrease) contributes strongly to the changes in pH simulated in response to climate change, and largely explains the contrast in magnitude between freshening and salinifying regions (Figure 4). In particular, the hydrological effect contributes to the

240   acidification in 'fresh-get-fresher' regions such as subpolar oceans, but opposes acidification in 'salty-get-saltier' regions such as the subtropical Atlantic (-0.001 vs. +0.002 on average over freshening and salinifying regions; grey bars in Figure 4c). Note that the climate-driven increase in pH simulated in the equatorial Pacific upwelling region cannot be accounted for by the hydrological effect (Figure 4a-b), but is instead associated with the weakened upwelling of cold and high-DIC waters simulated in this region(Figures 1b and 2a).
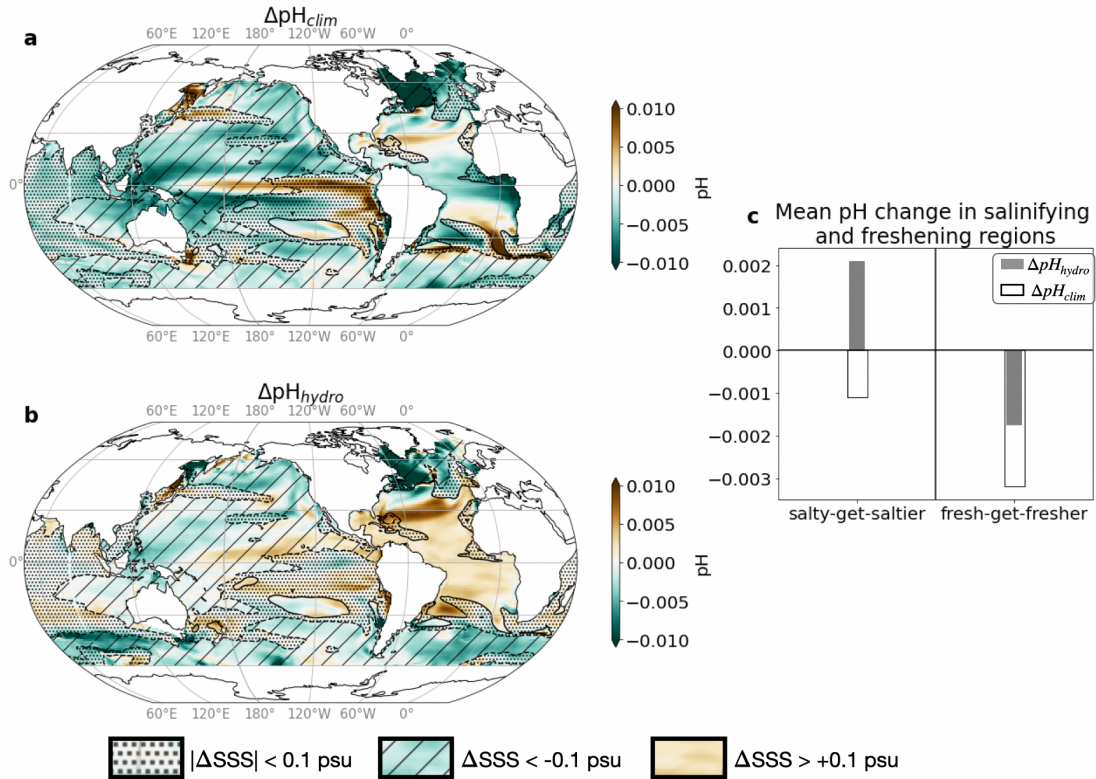
Figure 4. pH response to climate and hydrological effects. (a) Change in surface pH due to the climate effect (Standard minus Fix-Clim experiments) and (b) hydrological effect (Standard minus Fix-SSS experiments). Hatching indicates freshening ΔSSS_{hydro} <-0.1 while no hatching indicates salinity increase ΔSSS_{hydro} >0.1. Black contours indicate ΔSSS_{hydro} = +/-0.1 psu and stippling indicates regions with small salinity changes, which are not considered in our analysis ($|\Delta SSS_{hydro}|$ < 0.1 psu). (c) Mean change in salinifying (left, ΔSSS_{hydro} > 0.1 psu) and freshening (right, ΔSSS_{hydro} < -0.1 psu) regions outlined in maps, with empty bars representing the climate effect and solid bars representing the hydrological effect. See Table 3 for definitions.
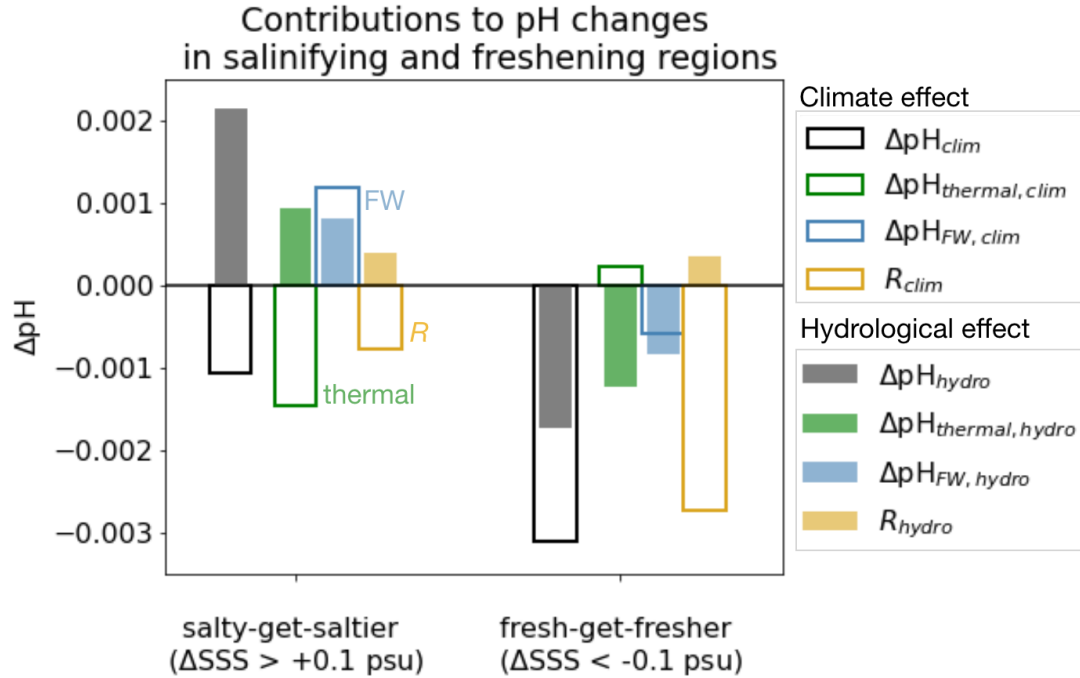
Figure 5. Thermal and freshwater components of pH changes in 'fresh-get-fresher' and 'salty-get-saltier' regions. Change in surface pH in the climate effect (empty bars) and the hydrological effect (filled bars), in 'salty-get-saltier' and 'fresh-get-fresher' regions (as shown in Figure 1). Black and grey bars represent total simulated pH change and are identical to those in Figure 4c. Blue bars represent contribution of freshwater effect (via dilution of DIC and Alkalinity). Green bars represent contribution of thermal effect (via SST change and DIC change due to SST). Yellow bars represent the residual (the difference between the sum of green + blue, and the actual change represented by black and grey bars). See Table 3 for definition of components.

We next interpret these pH changes due to the climate and hydrological effects in terms of a thermal effect (which includes the opposing effects of DIC and SST on pH) and a freshwater flux effect (which includes the opposing effects of DIC and Alkalinity on pH), using the thermal and freshwater components of DIC and Alkalinity changes presented in Section 3 (Figure 5).

The weakened acidification tied to the hydrological cycle in salinifying waters (i.e. an increase in pH tied to the hydrological effect) is attributed almost equally to the freshwater and thermal effects (filled bars in Figure 5). pH has a similar sensitivity to both Alkalinity and DIC in the modern surface ocean, and $\Delta\mathrm{Alk}_{FW}$ always exceeds $\Delta\mathrm{DIC}_{FW}$ (since the FW contribution scales with the mean value, and the mean Alkalinity concentration is higher than the mean DIC concentration; see Methods). As as result, the increasing $\Delta\mathrm{Alk}_{FW}$ drives a positive $\Delta\mathrm{pH}_{FW}$ in salty-get-saltier waters (Figure 6c). At the same time, hydrological cycle amplification drives a weak surface cooling (Liu et al., 2021) which further increases pH (McNeil and Matear, 2007). At lower latitudes where salty-get-saltier waters are found, the direct effect of cooling (cooling increases
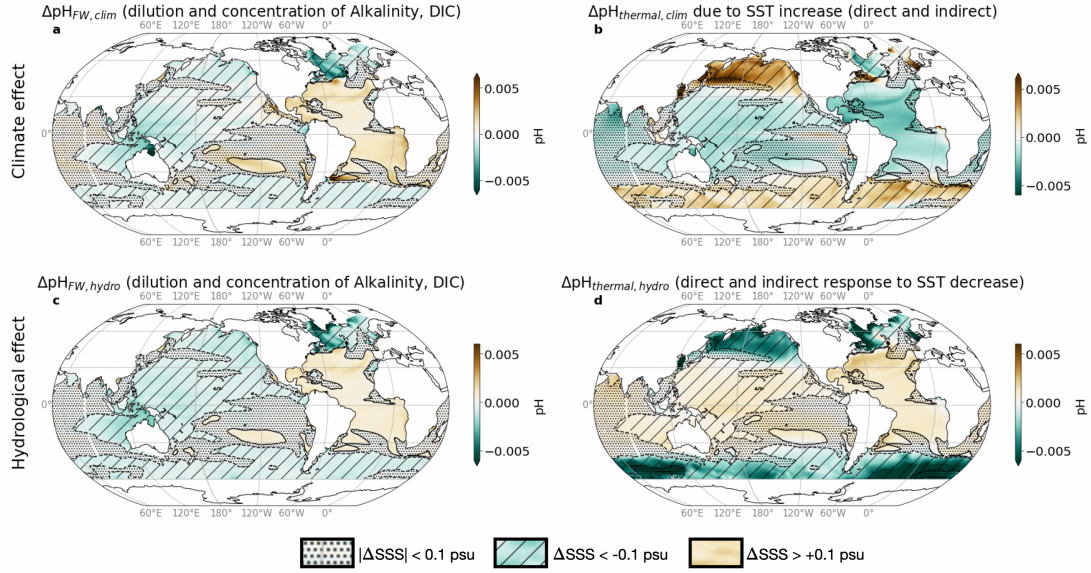
Figure 6. Contributions of temperature and freshwater flux changes to climate and hydrological effect. Upper row shows the contributions of (a) freshwater fluxes and (b) surface temperature change (warming) to the climate effect. Lower row shows the contributions of (c) freshwater fluxes and (d) surface temperature change (less warming) to the climate effect. Black contours indicate ΔSSS_{hydro} = +/-0.1 psu, hatching indicates ΔSSS_{hydro} <-0.1, no hatching indicates ΔSSS_{hydro} >0.1. See Table 3 for definitions.

pH) overcomes the indirect effect (cooling increases DIC and reduces pH). Together, the increased Alkalinity and decreased temperature increase pH, weakening the net acidification in the total climate effect. Similarly, the enhanced acidification in freshening waters is also attributed almost equally to the freshwater and thermal effects (filled bars in Figure 5). The decrease in alkalinity due to freshwater input reinforces acidification. In this case, the indirect effect of cooling on pH exceeds the direct effect leading additional to acidification, in particular in cold, DIC-rich high latitude waters, where the fresh-get-fresher signal is strongest (Figure 6 d).

This decomposition into freshwater and thermal effects is insightful but simplistic. The combined freshwater and thermal effects correctly predict the sign of pH changes, but better reconstruct the magnitude of the hydrological effect than of the climate effect (yellow residuals greater for climate effect in Figure 5). The sum of these two components underestimates the magnitude of the total simulated pH decrease in the climate effect (predicting a weak decrease relative to the simulated ΔpH_{clim} -0.001 and -0.003 in salinifying and freshening regions). The weakened air-sea CO_2 flux cannot explain the enhanced acidification, suggesting that this inaccuracy is related to error in our reconstructions of $\Delta Alk_{FW,clim}$, $\Delta DIC_{FW,clim}$, and $\Delta DIC_{thermal,clim}$, which are discussed above, as well as the covariation between drivers of pH changes which reflects the non-linearity of the carbonate chemistry system.

Despite these limitations, the hydrological effect appears to contribute strongly to the spatial pattern of pH changes. The discrepancy in pH changes between the salty-get-saltier and fresh-get-fresher regions due to hydrological cycle amplification

(nearly 0.004) is in fact larger than the discrepancy in the total climate effect (0.002). The hydrological effect introduces this strong pattern by (i) cooling the surface and (ii) freshwater dilution in freshening regions and concentration in salinifying regions.

4   Discussion and conclusions

Our results suggest that the changes in Alkalinity, DIC, and pH linked to hydrological cycle amplification contribute as strongly to the spatial pattern of the climate effect as warming alone, although these effects largely offset one another in the global mean. In fact, since Alkalinity is not strongly influenced by temperature, nearly the entire climate effect in surface Alkalinity is accounted for by the hydrological effect, i.e. dilution or concentration by anomalous freshwater fluxes (precipitation - evaporation). The climate effect includes a surprising DIC and pH increase (opposite the decreases expected from surface warming) in the subtropical Atlantic Ocean, as well as an exceptionally strong DIC decrease at higher latitudes. Both of these features can be largely accounted for with the hydrological effect. Although the freshwater loss from the ('salty-get-saltier') subtropical Atlantic Ocean leads to an increase in both Alkalinity and DIC, the increase in Alkalinity is greater (and the DIC increase is weakened by the global cooling effect of hydrological cycle amplification), leading to a local increase in pH. The critical role of Alkalinity in determining the response of marine carbonate chemistry to climate change here is consistent with prior studies (e.g. Chikamoto et al., 2023; Planchat et al., 2024). At high latitudes, the decrease in DIC associated with warming in the total climate effect is amplified by dilution ('fresh-get-fresher'), and tends to support stronger acidification. The nonlinear response of pH and other biologically important parameters (such as aragonite/calcite saturation states (e.g. Pinsonneault et al., 2012)) are left to other studies to study in more detail.

Although this is the first study to isolate the hydrological effect on seawater carbonate chemistry, the amplification of the hydrological cycle itself, and its impact on ocean heat uptake and SST, have been shown to be consistent across ocean-atmosphere models, despite differences in core ocean and atmosphere components (Williams et al., 2007; Liu et al., 2021; Held and Soden, 2006). Because of these prior results, we expect the sign and magnitude of these results to remain similar across other models. This study attempts to explain the mechanisms driving patterns in the total climate effect for DIC, Alkalinity, and pH, and is intended to complement two recent studies of the influence of the hydrological effect on ocean heat uptake and ocean oxygen distribution (Liu et al., 2021; Hogikyan et al., 2024). We find regional changes due to the hydrological effect alone are the same order of magnitude as the total climate effect and can explain the spatial patterning in the climate effect (+/- 0.01 pH, +/-20μmol kg^{-1} DIC, and +/-20 μmol kg^{-1} Alk), but both are of course smaller than the direct effect of CO$_2$ (in these simulations, approximately -0.2 pH, 120 μmol kg^{-1} DIC, and 20 μmol kg^{-1} Alk) (Williams et al., 2019). However, it is encouraging that we are able to clearly quantify this effect of freshwater fluxes even under relatively strong atmospheric CO$_2$ forcing, despite the strong non-linearity of ocean carbonate chemistry.

The surface patterns in DIC and Alkalinity presented here affect the distribution of carbon storage within the ocean. For example, the hydrological cycle leads to a slight increase in carbon storage in Mode and Intermediate Waters at the expense of deeper water masses, while the total climate effect tends to decrease carbon uptake and storage everywhere. However, these

305 changes (due to the total climate effect or the hydrological effect alone) are small in the ocean interior (generally $< |5| \; \mu$mol kg^{-1}).

Finally, it is worthwhile to note that our 'freshwater' component is similar to the traditional salinity normalization, in that both make use of the fact that freshwater fluxes should change DIC and Alkalinity approximately in proportion to salinity. However, we reference a spatially resolved pre-industrial control salinity to describe the effect of climate change rather than

310 referencing the central estimates of 1900 umol/kg DIC, 2310 umol/kg Alk, and 35 psu used in the standard normalization (Broecker and Peng, 1992). Our method makes fewer assumptions and is slightly more precise, but requires more data. Our study also demonstrates that this 'freshwater effect' (which the salinity normalization is intended to remove) can have substantial consequences for carbonate chemistry, with implications for CO_2 fluxes, pH, etc. This result raises the question of how useful salinity-normalized values are. If one only examined the salinity-normalized CO_2, for example, one might struggle to

315 explain changes in other carbonate system parameters, especially in a scenario with strong freshwater fluxes.

Code and data availability. Processed model results and code to reproduce figures are on Zenodo at DOI 10.5281/zenodo.13152692.

Appendix A
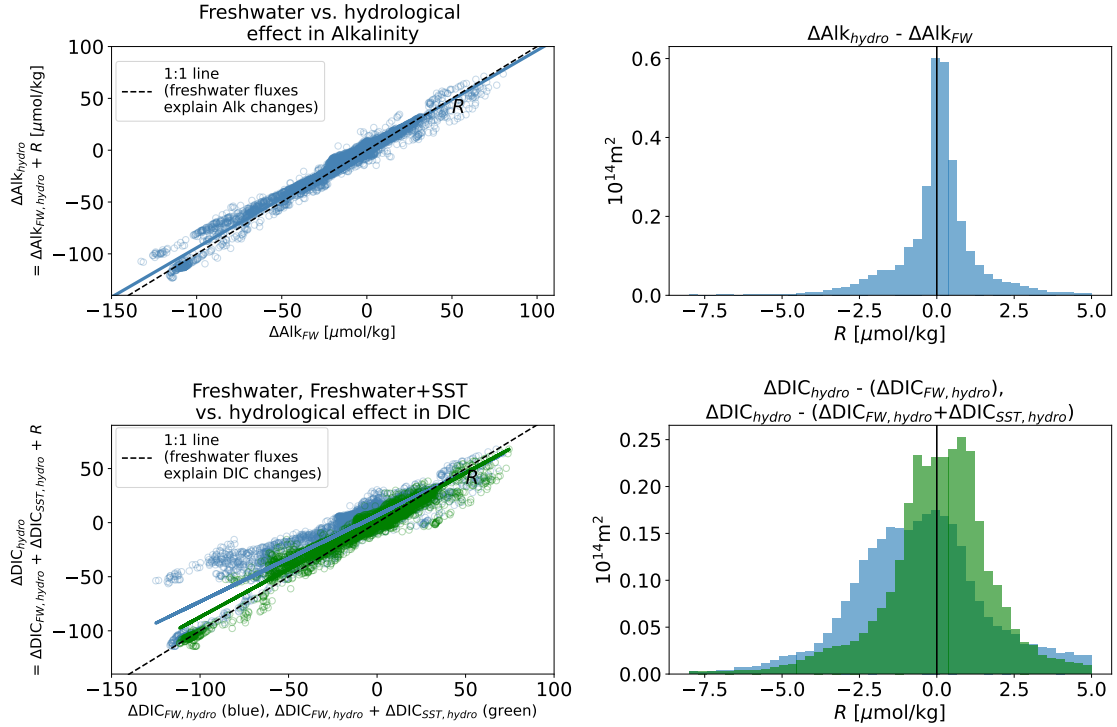
Figure A1. Ability of freshwater, SST decomposition to reconstruct spatial pattern of changes in surface DIC and Alkalinity with hydrological effect. Success of 'freshwater effect' ($\Delta\text{Alk}_{FW,hydro}$) in predicting ΔAlk_{hydro} (top), and success of 'freshwater + SST effects' ($\Delta\text{DIC}_{FW,hydro}+\Delta\text{DIC}_{SST,hydro}$) in predicting ΔDIC_{hydro} (bottom). Left hand side: scatter and unweighted regression of simulated surface ΔAlk_{hydro} or ΔDIC_{hydro} against the Δ_{hydro} predicted by our decomposition (for Alkalinity, $\Delta\text{Alk}_{FW,hydro}$; for DIC, $\Delta\text{DIC}_{FW,hydro}$ in blue and $\Delta\text{DIC}_{FW,hydro}+\Delta\text{DIC}_{SST,hydro}$ in green), at each surface location. Scatter around the fit is the error R. Right hand distributions represent area weighted values of R for Alkalinity (top) and DIC (bottom).
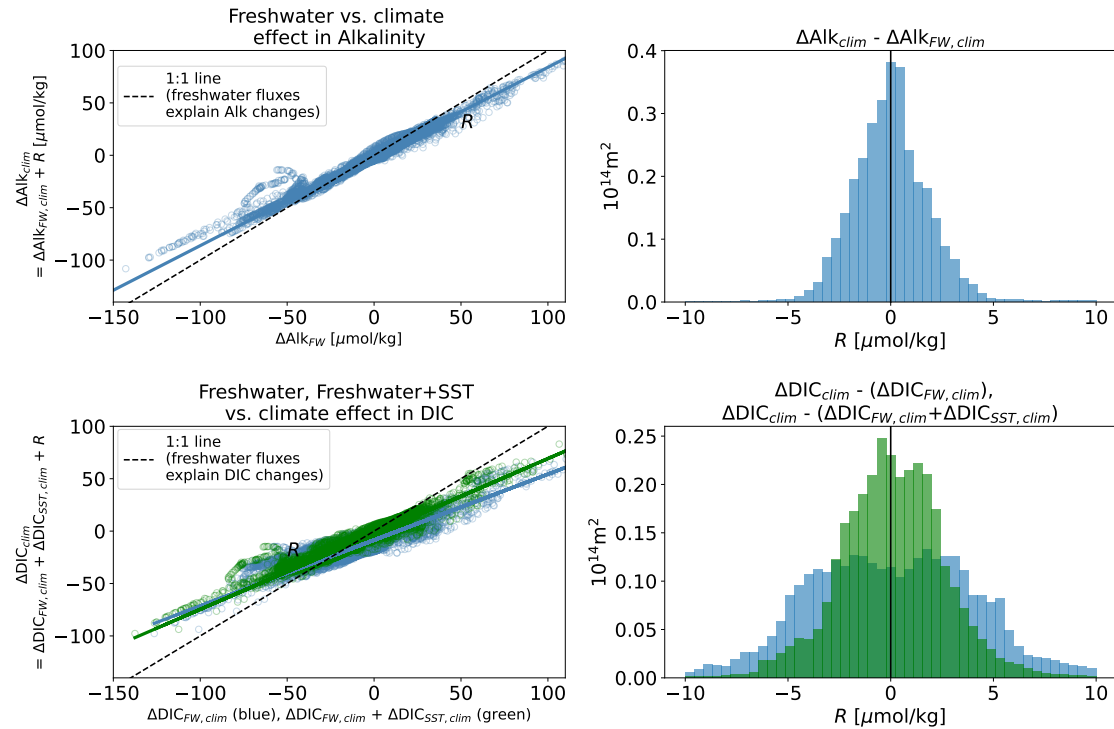
Figure A2. Ability of freshwater, SST decomposition to reconstruct spatial pattern of changes in surface DIC and Alkalinity with climate effect. As in Figure A1 but for the climate effect. The greater disagreement here is primarily due to anomalous fluxes.
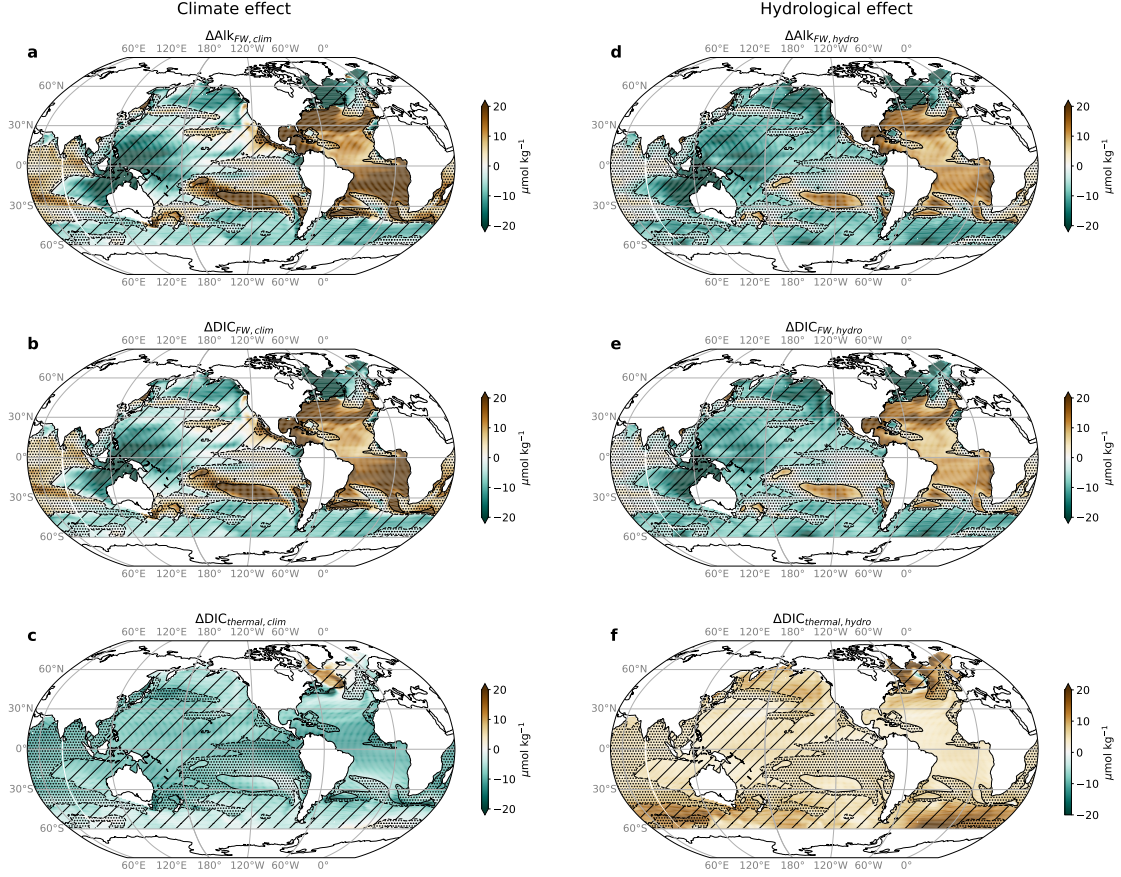
Figure A3. Thermal and freshwater components of DIC and Alkalinity changes. (a-c) change attributed to freshwater ($\Delta\text{Alk}_{FW,clim} = f_{FW,clim}\text{Alk}_{Fix-Clim}$, $\Delta\text{DIC}_{FW,clim} = f_{FW,clim}\text{DIC}_{Fix-Clim}$) and thermal ($\Delta\text{DIC}_{thermal,clim}$ = -7ΔSST_{clim}) components in climate effect; (d-f) change attributed to freshwater ($\Delta\text{Alk}_{FW,hydro} = f_{FW,hydro}\text{Alk}_{Fix-SSS}$, $\Delta\text{DIC}_{FW,hydro} = f_{FW,hydro}\text{DIC}_{Fix-SSS}$) and thermal ($\Delta\text{DIC}_{thermal,hydro}$ = -7ΔSST_{hydro}) components in hydrological effect.
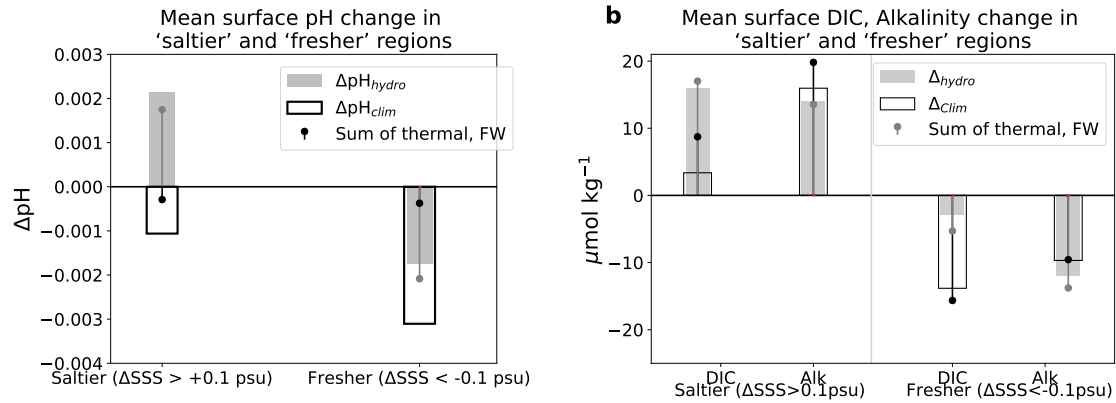
Figure A4. Error in our estimation of pH, DIC, Alk changes, averaged over 'salty-get-saltier' and 'fresh-get-fresher' regions. Bars of pH change in (a) are identical to those in Figure 4c, while bars of DIC, Alk change in (b) are identical to those in Figure 2e (i.e. empty black bars correspond to the climate effect while the grey filled bars correspond to the hydrological effect). Lollipops make a comparison between the estimate from our decomposition, and the full changes simulated by ESM2M (represented by the bars). Grey lollipops represent $\Delta X_{FW,Hydro} + \Delta X_{thermal,Hydro}$ (X is pH, DIC, or Alk), and the difference between the grey bars and lollipops is R_{Hydro}. Black lollipops represent $\Delta X_{FW,Clim} + \Delta X_{thermal,Clim}$ (X is pH, DIC, or Alk), and the difference between the black bars and lollipops is R_{Clim}. Please see Methods and Tables **??** for calculations of FW, thermal components of pH, DIC, Alk.
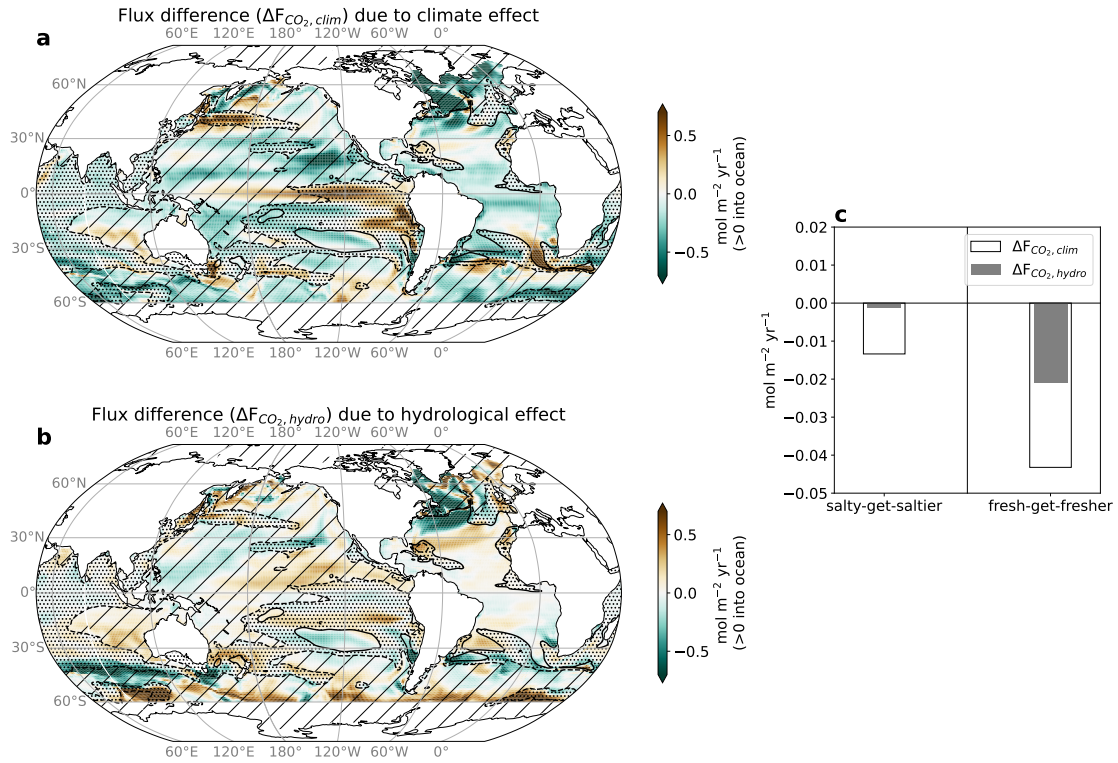
Figure A5. Air-sea flux of CO$_2$, difference due to (a) climate effect and (b) hydrological effect. Stippling where ΔSSS_{hydro} is small, as in Figures 1, 2, 4, 5.

Author contributions. A.H. contributed to design and execution of experiments, data analysis, and writing. L.R. contributed to design of experiments and writing.

320 *Competing interests.* The authors declare no competing interests.

Acknowledgements. A.H. acknowledges support from the National Science Foundation Graduate Research Fellowship Program under Grant No. DGE-2039656. Any opinions, findings, and conclusions or recommendations expressed in this material are those of the author and do not necessarily reflect the views of the National Science Foundation. The authors thank the Princeton Institute for Computational Science and Engineering (PICSciE) for High Performance Computing (HPC) provision, storage and support.

325 **References**

Arora, V. K., Boer, G. J., Friedlingstein, P., Eby, M., Jones, C. D., Christian, J. R., Bonan, G., Bopp, L., Brovkin, V., Cadule, P., et al.: Carbon–concentration and carbon–climate feedbacks in CMIP5 Earth system models, Journal of Climate, 26, 5289–5314, 2013.

Broecker, W. S. and Peng, T.-H.: Interhemispheric transport of carbon dioxide by ocean circulation, Nature, 356, 587–589, 1992.

Caldeira, K. and Wickett, M. E.: Anthropogenic carbon and ocean pH, Nature, 425, 365–365, 2003.

330 Cheng, L., Trenberth, K. E., Fasullo, J., Boyer, T., Abraham, J., and Zhu, J.: Improved estimates of ocean heat content from 1960 to 2015, Science Advances, 3, e1601 545, 2017.

Chikamoto, M. O., DiNezio, P., and Lovenduski, N.: Long-Term Slowdown of Ocean Carbon Uptake by Alkalinity Dynamics, Geophysical Research Letters, 50, e2022GL101 954, 2023.

Doney, S. C., Busch, D. S., Cooley, S. R., and Kroeker, K. J.: The impacts of ocean acidification on marine ecosystems and reliant human
335 communities, Annual Review of Environment and Resources, 45, 83–112, 2020.

Dunne, J. P., John, J. G., Adcroft, A. J., Griffies, S. M., Hallberg, R. W., Shevliakova, E., Stouffer, R. J., Cooke, W., Dunne, K. A., Harrison, M. J., et al.: GFDL's ESM2 global coupled climate–carbon earth system models. Part I: Physical formulation and baseline simulation characteristics, Journal of climate, 25, 6646–6665, 2012.

Dunne, J. P., John, J. G., Shevliakova, E., Stouffer, R. J., Krasting, J. P., Malyshev, S. L., Milly, P., Sentman, L. T., Adcroft, A. J., Cooke,
340 W., et al.: GFDL's ESM2 global coupled climate–carbon earth system models. Part II: carbon system formulation and baseline simulation characteristics, Journal of Climate, 26, 2247–2267, 2013.

Durack, P. J. and Wijffels, S. E.: Fifty-year trends in global ocean salinities and their relationship to broad-scale warming, Journal of Climate, 23, 4342–4362, 2010.

Durack, P. J., Wijffels, S. E., and Matear, R. J.: Ocean salinities reveal strong global water cycle intensification during 1950 to 2000, science,
345 336, 455–458, 2012.

Friedlingstein, P. and Prentice, I.: Carbon–climate feedbacks: a review of model and observation based estimates, Current Opinion in Environmental Sustainability, 2, 251–257, 2010.

García-Ibáñez, M. I., Zunino, P., Fröb, F., Carracedo, L. I., Ríos, A. F., Mercier, H., Olsen, A., and Pérez, F. F.: Ocean acidification in the subpolar North Atlantic: rates and mechanisms controlling pH changes, Biogeosciences, 13, 3701–3715, 2016.

350 Gattuso, J. P., Hoegh-Guldberg, O., and Pörtner, H.: Cross-chapter box on coral reefs, in: Climate Change 2014: Impacts, Adaptation, and Vulnerability. Part A: Global and Sectoral Aspects. Contribution of Working Group II to the Fifth Assessment Report of the Intergovernmental Panel of Climate Change, pp. 97–100, Cambridge University Press, 2014.

Held, I. M. and Soden, B. J.: Robust responses of the hydrological cycle to global warming, Journal of climate, 19, 5686–5699, 2006.

Hogikyan, A., Resplandy, L., Liu, M., and Vecchi, G.: Hydrological cycle amplification reshapes warming-driven oxygen loss in the Atlantic
355 Ocean, Nature climate change, pp. 1–9, 2024.

Humphreys, M. P., Lewis, E. R., Sharp, J. D., and Pierrot, D.: PyCO2SYS v1. 8: Marine carbonate system calculations in Python, Geoscientific Model Development, 15, 15–43, 2022.

Katavouta, A. and Williams, R. G.: Ocean carbon cycle feedbacks in CMIP6 models: contributions from different basins, Biogeosciences, 18, 3189–3218, 2021.

360 Kroeker, K. J., Kordas, R. L., Crim, R., Hendriks, I. E., Ramajo, L., Singh, G. S., Duarte, C. M., and Gattuso, J.-P.: Impacts of ocean acidification on marine organisms: quantifying sensitivities and interaction with warming, Global change biology, 19, 1884–1896, 2013.

Liu, M., Vecchi, G., Soden, B., Yang, W., and Zhang, B.: Enhanced hydrological cycle increases ocean heat uptake and moderates transient climate change, Nature climate change, 11, 848–853, 2021.

Lovenduski, N. S., Gruber, N., and Doney, S. C.: Toward a mechanistic understanding of the decadal trends in the Southern Ocean carbon sink, Global Biogeochemical Cycles, 22, 2008.

Manabe, S. and Stouffer, R. J.: Simulation of abrupt climate change induced by freshwater input to the North Atlantic Ocean, Nature, 378, 165–167, 1995.

Manabe, S. and Wetherald, R. T.: The effects of doubling the CO_2 concentration on the climate of a general circulation model, Journal of Atmospheric Sciences, 32, 3–15, 1975.

McNeil, B. I. and Matear, R. J.: Climate change feedbacks on future oceanic acidification, Tellus B: Chemical and Physical Meteorology, 59, 191–198, 2007.

Menary, M. B. and Wood, R. A.: An anatomy of the projected North Atlantic warming hole in CMIP5 models, Climate Dynamics, 50, 3063–3080, 2018.

Pilcher, D. J., Naiman, D. M., Cross, J. N., Hermann, A. J., Siedlecki, S. A., Gibson, G. A., and Mathis, J. T.: Modeled effect of coastal biogeochemical processes, climate variability, and ocean acidification on aragonite saturation state in the Bering Sea, Frontiers in Marine Science, 5, 508, 2019.

Pinsonneault, A., Matthews, H. D., Galbraith, E., and Schmittner, A.: Calcium carbonate production response to future ocean warming and acidification, Biogeosciences, 9, 2351–2364, 2012.

Planchat, A., Bopp, L., Kwiatkowski, L., and Torres, O.: Carbonate pump feedbacks on alkalinity and the carbon cycle in the 21st century and beyond, EGUsphere, https://doi.org/https://doi.org/10.5194/egusphere-2023-1218, 2024.

Pörtner, H.-O.: Integrating climate-related stressor effects on marine organisms: unifying principles linking molecule to ecosystem-level changes, Marine Ecology Progress Series, 470, 273–290, 2012.

Rayner, N., Parker, D. E., Horton, E., Folland, C. K., Alexander, L. V., Rowell, D., Kent, E. C., and Kaplan, A.: Global analyses of sea surface temperature, sea ice, and night marine air temperature since the late nineteenth century, Journal of Geophysical Research: Atmospheres, 108, 2003.

Sarmiento, J. L.: Ocean biogeochemical dynamics, Princeton university press, 2006.

Schwinger, J., Tjiputra, J. F., Heinze, C., Bopp, L., Christian, J. R., Gehlen, M., Ilyina, T., Jones, C. D., Salas-Mélia, D., Segschneider, J., et al.: Nonlinearity of ocean carbon cycle feedbacks in CMIP5 earth system models, Journal of Climate, 27, 3869–3888, 2014.

Siedlecki, S., Salisbury, J., Gledhill, D., Bastidas, C., Meseck, S., McGarry, K., Hunt, C., Alexander, M., Lavoie, D., Wang, Z., et al.: Projecting ocean acidification impacts for the Gulf of Maine to 2050: New tools and expectations, Elem Sci Anth, 9, 00 062, 2021.

Williams, P. D., Guilyardi, E., Sutton, R., Gregory, J., and Madec, G.: A new feedback on climate change from the hydrological cycle, Geophysical research letters, 34, 2007.

Williams, R. G., Katavouta, A., and Goodwin, P.: Carbon-cycle feedbacks operating in the climate system, Current Climate Change Reports, 2019.